Short title: ONAC127 and ONAC129 regulate rice grain filling

A Heat Stress Responsive NAC Transcription Factor Heterodimer Plays Key Roles in Rice Caryopsis Filling

Ye Ren, Zhouquan Huang, Hao Jiang, Zhuo Wang, Fengsheng Wu, Yufei Xiong, Jialing Yao *

College of Life Science and Technology, Huazhong Agricultural University, Wuhan 430070, China.

Corresponding author: Jialing Yao, Ph.D. and Professor, College of Life Science and Technology, Huazhong Agricultural University, Wuhan 430070, China.

* Address correspondence to yaojlmy@mail.hzau.edu.cn

Telephone: 86-27-87282866

Fax: 86-27-87282866

ABSTRACT

High temperature usually leads to the failure of grain filling during caryopsis development, resulting in the loss of yield, however the mechanism is not yet well elucidated. Here, we report that two rice caryopsis-specific NAM/ATAF/CUC domain transcription factors, *ONAC127* and *ONAC129*, respond to heat stress and are involved in the caryopsis filling process. *ONAC127* and *ONAC129* are dominantly expressed in pericarp during grain filling and can form a heterodimer. To investigate the functions of these two ONACs, we obtained CRISPR/cas9 induced mutants and overexpression lines of them. Interestingly, we found that both knock-out and overexpression plants showed incompletely filling and shrunken phenotype of caryopses, which became more severe under heat stress. The shrunken caryopses of these transgenic lines are usually with ectopic accumulation of starch in the pericarp. Transcriptome analyses revealed that *ONAC127* and *ONAC129* mainly regulate stimulus response, cell wall construction and nutrient transport etc. ChIP-seq analyses identified the direct targets of ONAC127 and ONAC129 in developing caryopses, including monosaccharide transporter *OsMST6*, sugar transporter *OsSWEET4*, calmodulin-like protein *OsMSR2* and Ethylene-Response AP2/ERF Factor *OsEATB*. The result suggested that *ONAC127* and *ONAC129* might regulate the caryopsis filling through sugar transportation and abiotic stress responses. Overall, this study demonstrates the transcriptional regulatory networks involving ONAC127 and ONAC129, which coordinates multiple pathways to modulate caryopsis development and heat stress response at rice filling stage.

44 **INTRODUCTION**

45 Rice caryopsis development starts from the fertilized ovary and finishes with a
46 dehydrated, hard and transparent grain. This process can be divided into three stages by
47 landmark events: cell division, organogenesis and maturation. (Agarwal et al., 2011). A
48 rice caryopsis is mainly composed of endosperm filled with starch grains, and the
49 biosynthesis of starch is closely related to carbohydrates transportation. Carbohydrates
50 are synthesized in leaves and delivered to caryopses via phloem (Patrick, 1997), then
51 unloaded to the pericarp as the energy and materials for starch biosynthesis (Zhang et
52 al., 2007). The dorsal vascular bundle passes through the pericarp is the main nutrient
53 transport tissue in caryopsis (Oparka and Gates, 1981). While the vascular bundles are
54 not contiguous with endosperm tissue (Hoshikawa, 1984), the apoplasmic pathway is
55 the only way for nutrient to reach the starchy endosperm. (Matsuda et al., 1979).

56 Carbohydrates may enter the nucellar epidermis directly through plasmodesmata,
57 then be transported to the apoplasmic space with sugar transporter protein OsSWEETs
58 (sugar will eventually be exported transporters) and partially hydrolyzed into
59 monosaccharide by cell wall invertase OsCINs. The monosaccharide is transported into
60 the aleurone layer mainly by monosaccharide transporter OsMSTs while the rest un-
61 hydrolyzed sucrose is directly transported into the aleurone layer via sucrose transporter
62 OsSUTs (Yang et al., 2018). The nutrient transportation is also regulated by a range of
63 transcription factors such as *OsNF-YB1* and *OsNF-YC12*, which activate the expression
64 of OsSUTs to capture the leaked sucrose in apoplasmic space. Knockout of *NF-YB1* or
65 *OsNF-YC12* leads to defective grains with chalky endosperms and similar phenotype
66 has been observed in mutants of *OsSUT1* (Bai et al., 2016; Xiong et al., 2019).

67 The nutrient transport processes in caryopsis are susceptible to changing
68 environmental conditions, extreme external stimuli (especially the extreme temperature)
69 during grain-filling stage will lead to a reduction of nearly 50% in rice (Hu and Xiong,
70 2014). Plants respond to the unexpected high temperature through some stress-specific
71 signaling pathways. During heat stress signal transduction, the heat shock transcription

72 factors (HSFs) will be activated to regulate the expression of downstream heat shock
73 proteins (HSPs) and other stress-related genes. For example, AP2/EREBP transcription
74 factor *DREB2A* can activate a heat shock transcription factor *hsfA3* under heat stress to
75 induce the expression of specific HSPs (Schramm et al., 2008). Similarly, the
76 expression of *OsbZIP60*, which play important roles in moisture retention and heat-
77 damage resistance, is induced under heat stress and endoplasmic reticulum stress (Oono
78 et al., 2010). Although several plant heat stress response related proteins have been
79 found and elucidated, the mechanisms of the response are still poorly understood.

80 NAC (NAM, ATAF1/2, CUC2) transcription factors are one of the largest family
81 of plant specific transcription factors with 151 members in rice (Nuruzzaman et al.,
82 2010). The typical structure of NAC transcription factors is a conserved NAC domain
83 with about 150 amino acids in N-terminus, followed by a variable transcriptional
84 regulation region (TRR) in C-terminus (Christianson et al., 2010). The NAC domain
85 can be further subdivided into five subdomains [A-E], subdomains C and D are highly
86 conserved and may mainly act in DNA-binding (Ooka et al., 2003). In addition, some
87 subdomain D contains a hydrophobic NAC repression domain (NARD) which can
88 suppress the transcriptional activity of NAC transcription factors by suppressing their
89 DNA-binding ability or nuclear localization ability. The specific functional motif in
90 NARD, LVFY can suppress not only the activity of NAC transcription factors, but also
91 the other transcription factors by its hydrophobicity (Hao et al., 2010).

92 NAC transcription factors are involved in many biological processes in plants, such
93 as organ development, secondary wall synthesis, stress response and so on. For instance,
94 *NAC29* and *NAC31* regulate downstream cellulose synthase (CESA) by activating the
95 downstream transcription factor *MYB61* to control the synthesis of secondary wall
96 (Huang et al., 2015). For stress response, especially in abiotic ways, the NAC
97 transcription factors are master regulators in this process. *RD26* gene is the first NAC
98 transcription factor identified as a regulator in mediating abscisic acid (ABA) and
99 jasmonate (JA) signaling during stress responses in Arabidopsis (Fujita et al., 2004).

100 *SNAC1* is a stress-responsive NAC transcription factor confers rice drought tolerance
101 by closing stomata (Hu et al., 2006) and *SNAC3* confers heat and drought tolerance
102 through regulation of reactive oxygen species (Fang et al., 2015). *OsNAC2* is also
103 reported involving in drought stress response mediated by ABA (Shen et al., 2017).
104 Meanwhile, it plays divergent roles in different biological processes, such as regulating
105 shoot branching (Mao et al., 2007), affecting plant height and flowering time through
106 mediating the gibberellic acid (GA) pathway (Chen et al., 2015). *VNI2* in Arabidopsis
107 is a bifunctional NAC transcription factor reported as a transcriptional repressor
108 functioning in xylem vessel formation (Yamaguchi et al., 2010), but the transcriptional
109 activator activity of *VNI2* is induced by high salinity stress to regulate the leaf longevity
110 (Yang et al., 2011).

111 Nine caryopsis-specific NAC transcription factors were found through
112 transcriptome analyses in rice (Mathew et al., 2016).We selected four of these genes,
113 *ONAC025*, *ONAC127*, *ONAC128* and *ONAC129* for further analyses, which located in
114 the linked regions of chromosome 11 and were identified as a gene cluster (Fang et al.,
115 2008). As recent study implied two NAC transcription factors specifically expressed in
116 maize seeds, *ZmNAC128* and *ZmNAC130*, playing critical roles in starch and protein
117 accumulation in seeds filling (Zhang et al., 2019). We inferred that the four NAC
118 transcriptional factors might also be involved in some important processes in rice
119 caryopsis development. In this study, we selected *ONAC127* and *ONAC129* from the
120 four genes, which could form a heterodimer and participate in apoplasmic
121 transportation as well as heat stress response to regulate rice caryopsis filling. These
122 findings broadened the understanding of the regulation network of stress response and
123 grain filling in rice.

124 **RESULTS**

125 ***ONAC127* and *ONAC129* are specifically expressed in caryopsis**

126 To understand these four genes basically, we firstly checked the expression data of

127 *ONAC025*, *ONAC127*, *ONAC128* and *ONAC129* in the microarray database CREP
128 (http://crep.ncpgr.cn) (Wang et al., 2010). The data showed that the expression level of
129 *ONAC025* in caryopsis was significantly higher than that of the rest genes, while that
130 of *ONAC128* was the lowest among the four genes. For *ONAC127* and *ONAC129*, they
131 showed the highest expression level at 7 d after pollination (DAP) and then decreased
132 gradually, such similar expression pattern attracted our further attention.

133 For validating the spatial and temporal expression patterns and further exploring
134 the specific expression distribution of *ONAC127* and *ONAC129* in caryopsis, we
135 mechanically isolated rice caryopses at 5-14 DAP to the mixture of pericarp and
136 aleurone layer, starch endosperm and embryo for qRT-PCR analyses by the method
137 described by Bai (Bai et al., 2016). The aleurone layer specifically expressed gene
138 *oleosin* and the starch endosperm specifically expressed gene *SDBE* were used as
139 markers (Ishimaru et al., 2015) (Supplemental Fig. S1). The result showed that
140 *ONAC127* and *ONAC129* were mainly expressed in pericarp or aleurone layer while
141 they were weakly expressed in starch endosperm, and the expression went to the
142 summit at 5 DAP during the whole development process (Fig. 1A).

143 The mRNA *in situ* hybridization analyses using the unripe caryopses of ZH11
144 turned out that *ONAC127* and *ONAC129* were dominantly expressed in pericarp, when
145 the expression level in aleurone layer and starch endosperm were quite weak (Fig. 1B).
146 Histochemical GUS activity was also detected using the transgenic plants expressing
147 pONAC127::GUS and pONAC129::GUS, the result was almost identical to that of *in*
148 *situ* hybridization analyses, that *ONAC127* and *ONAC129* were preferentially
149 expressed in pericarp of caryopsis (Fig. 1C). Considering that 5 DAP is a key time point
150 of caryopsis development for the organogenesis is finished and maturation stage is just
151 initiated (Agarwal et al., 2011). *ONAC127* and *ONAC129* might be involved in some
152 substance exchange processes playing vital roles in caryopsis filling and maturation.

153 We then carried out the assay through transforming green fluorescent protein (GFP)
154 fused ONAC127 or ONAC129 protein into rice protoplast transiently to investigate the

155 subcellular localization pattern of the two genes. 35S::GFP was used as a positive
156 control and 35S::Ghd7-CFP was used as a nuclear marker (Xue et al., 2008). The
157 fluorescence generated by ONAC127-GFP and ONAC129-GFP was distributed in the
158 nucleus and cytoplasm just like the way positive control did (Fig. 1D). For further
159 confirming the subcellular localization, transgenic plants expressing pUbi::ONAC127-
160 GFP and pUbi::ONAC129-GFP were generated in Zhonghua11 (ZH11) background.
161 The subcellular localization pattern of ONAC127 and ONAC129 were validated by
162 detecting the fluorescence from the roots of two-week-old rice seedlings of the plants,
163 ONAC127 and ONAC129 proteins were indeed localized in the nucleus and cytoplasm
164 (Supplemental Fig. S2).

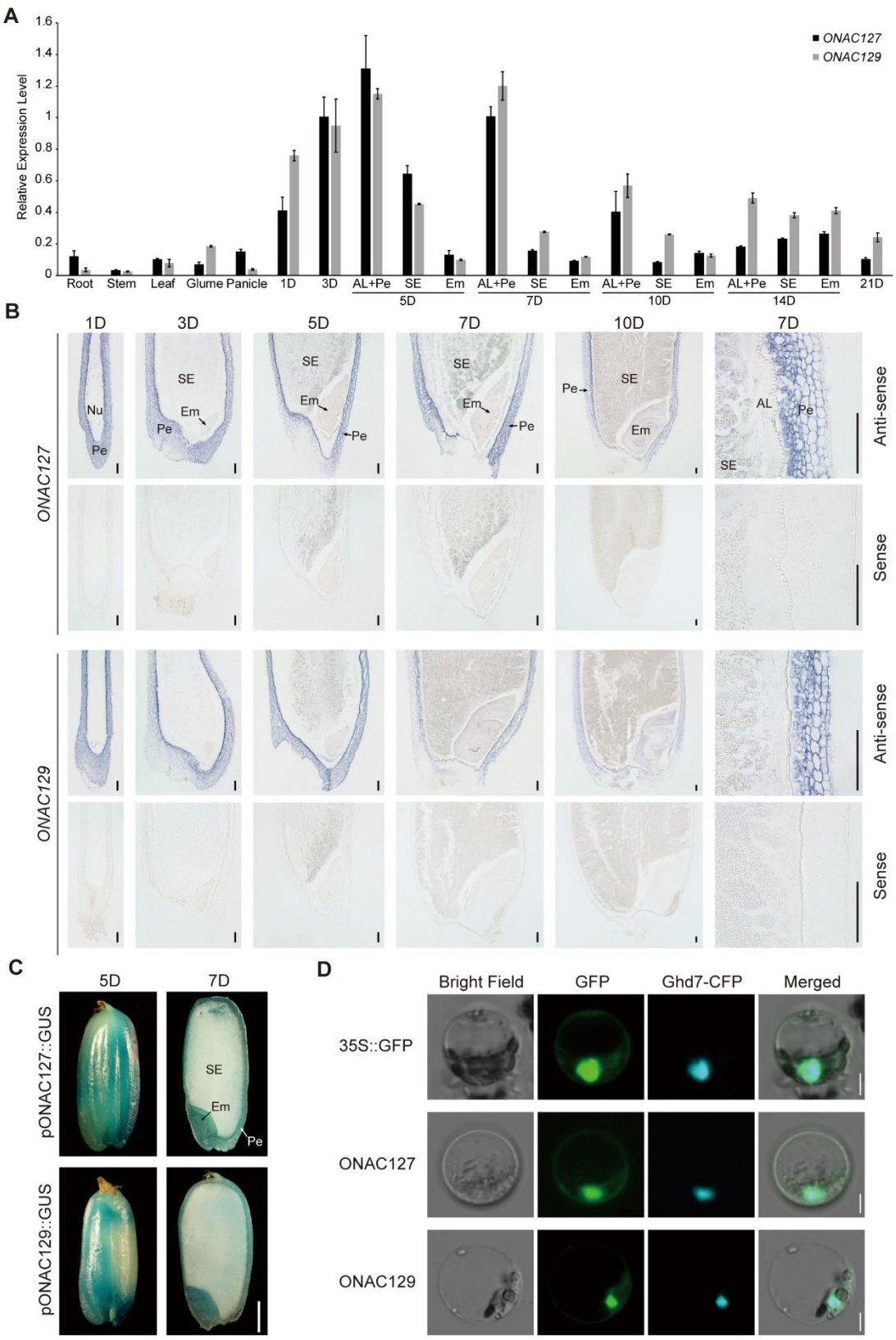

Fig. 1 Spatial and temporal expression patterns of *ONAC127* and *ONAC129*.

A. qRT-PCR analyses of *ONAC127* and *ONAC129* in different tissue. AL, aleurone layer; Pe, pericarp; SE, starchy endosperm; Em, embryo; 1-21D, caryopses collected during 1-21 DAP. The values in each

169 column are the mean of three technical replicates and the error bars indicate the ±SD. Ubiquitin is used
170 as the reference gene. B. *In situ* hybridization of sectioned caryopses collected at 1, 3, 5, 7 and 10 DAP
171 using anti-sense and sense probes. Nu, nucellar; Pe, pericarp; SE, starchy endosperm; Em, embryo; AL,
172 aleurone layer. Scale bars are 50 μm. C. Histochemical GUS activity detection using pONAC127::GUS
173 and pONAC129::GUS. Pe, pericarp; SE, starchy endosperm; Em, embryo. Scale bar is 1 mm. D.
174 Subcellular localization of the *ONAC127* and *ONAC129* in rice protoplasts. 35S::Ghd7-CFP is used as a
175 nuclear marker. Scale bars are 5 μm.

176 **ONAC127 and ONAC129 can form a heterodimer**

177 It was noticed that the NAC transcription factors usually function as a dimer (Olsen
178 et al., 2005), thus we investigated if there was any interaction between ONAC127 and
179 ONAC129. The result indicated that ONAC127 could interact with ONAC129 in yeast
180 (Fig. 2A). To confirm the interaction between ONAC127 and ONAC129, the *in vitro*
181 GST pull-down assay was carried out. His-tagged ONAC127 and GST-tagged
182 ONAC129 were expressed respectively and incubated together. The protein mixture of
183 GST and ONAC127-His was used as a negative control. After purification by
184 Glutathione Agarose, ONAC127-His was detected in the sample containing
185 ONAC129-GST instead of the control with His-tag antibody (Fig. 2B). The *in vivo*
186 bimolecular fluorescence complementation (BiFC) assay was also performed with rice
187 protoplasts. Nuclear homodimer OsbZIP63 was chosen as positive control (Walter et
188 al., 2004), and 35S::Ghd7-CFP was used as a nuclear marker. Yellow fluorescence
189 generated from the interaction between ONAC127-YFP^N and ONAC129-YFP^C was
190 detected, which confirmed the heterodimer ONAC127 and ONAC129 formed in
191 nucleus (Fig. 2C). In view of previous studies, some of NAC transcription factors were
192 located in the cytoplasm or plasma membrane first, and then were imported to nuclei
193 under some specific conditions (Fang et al., 2014). Considering the subcellular
194 localization pattern of ONAC127 and ONAC129 (Fig. 1D), we speculated that these
195 two proteins might also exert their transcriptional regulation functions in this way.

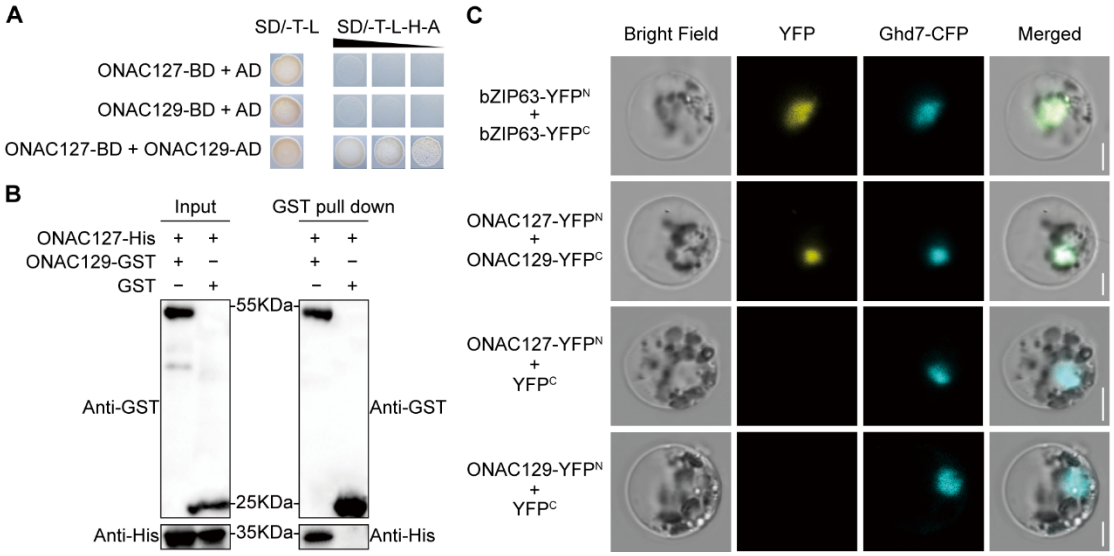

Fig. 2 Interaction between ONAC127 & ONAC129.

A. The yeast two-hybrid assay. The full-length cDNA of ONAC127 and ONAC129 are both cloned into pGBKT7 (BD) and pGADT7 (AD). The transformants are grown on [SD/–Trp /–Leu] and [SD/–Trp/–Leu/–His/–Ade] plates with 10^0, 10^{-1} and 10^{-2} fold dilution. B. The pull-down assays showing that there is a direct interaction between ONAC127-His and ONAC129-GST and *in vitro*. C. The BiFC assays of ONAC127 and ONAC129. ONAC127-YFP^N and ONAC129-YFP^C interact to form a functional YFP in rice protoplasts. 35S::Ghd7-CFP is used as a nuclear marker. Scale bars are 5 μm.

ONAC127 and *ONAC129* are key players in starch accumulation during rice caryopsis filling

We obtained the specifically knockout *ONAC127* or *ONAC129* mutants (*onac127* and *onac129*) in ZH11 background by CRISPR/Cas9 genome editing system (Ma et al., 2015). Considering that these two proteins could form a heterodimer, double knockout mutants (*onac127;129*) were also obtained. The sgRNA target sites were designed at the exons of *ONAC127* and *ONAC129* using the web-based tool CRISPR-P (Liu et al., 2017). There are two target sites of each gene, which were expected to generate different mutations in the coding region of the genes (Fig. 3A). The grains of three T_0 homozygous plants of each mutant were selected for generating independent T_1 transgenic lines. The sequencing data of the transgenic lines was decoded by the method described by Liu (Liu et al., 2015), and the genotypes of the homozygous lines were

216 showed in Supplemental Fig. S3. On the other hand, we also generated the
217 overexpression lines pUbi::ONAC127-FLAG and pUbi::ONAC129-FLAG (OX127
218 and OX129) (Fig. 3B). Relative expression level of the overexpression lines was
219 analyzed by qRT-PCR (Supplemental Fig. S4).

220 During the rice reproductive stage, we found the development of caryopses in
221 *ONAC127* and *ONAC129* transgenic lines arrested during 5-7 DAP (Supplemental Fig.
222 S5), resulting in shrunken and incompletely filled grains after ripening (Fig. 3C, D). As
223 we mentioned before, the expression level of *ONAC127* and *ONAC129* was very high
224 during 5-7 DAP (Fig. 1A), the functions of *ONAC127* and *ONAC129* seem to be closely
225 related to grain filling, especially at the early stage of maturation. Since the phenotype
226 is illogical, we detected the expression level of the two ONACs in the transgenic lines
227 immediately. It turned out that the expression of *ONAC127* and *ONAC129* was up-
228 regulated in the overexpression lines and down-regulated in the mutants indeed
229 (Supplemental Fig. S6). We speculated that ONAC127 and ONAC129 may regulate
230 several different pathways contributing to caryopsis filling at the same time. The
231 expression of the two ONACs may need to be maintained at a steady level, any
232 fluctuations in their expression would interfere the normal running of different
233 pathways and have the chance to bring caryopsis filling defection.

234 To investigate the reason of the shrunken phenotype further, histological analyses
235 through resin embedded sections were prepared with 7 DAP incompletely filling
236 caryopses. In ZH11, starch was stored transiently in the pericarp during the early stage,
237 the degradation of starch in the pericarp correlated with starch accumulation in the
238 endosperm (Wu et al., 2016). As we expected, the starch in the endosperm of ZH11
239 caryopses was arrayed neatly, densely and hardly found in pericarp (Fig. 3E). In
240 contrast, many starch grains accumulated in the pericarp of the mutants and the
241 overexpression lines of *ONAC127* and *ONAC129*, especially in the double mutant
242 *onac127;129*, in which substantial starch grains were hardly seen in endosperm (Fig.
243 3E). The finding above suggested that *ONAC127* and *ONAC129* might play critical

roles in starch translocation and mobilization towards the developing endosperm.

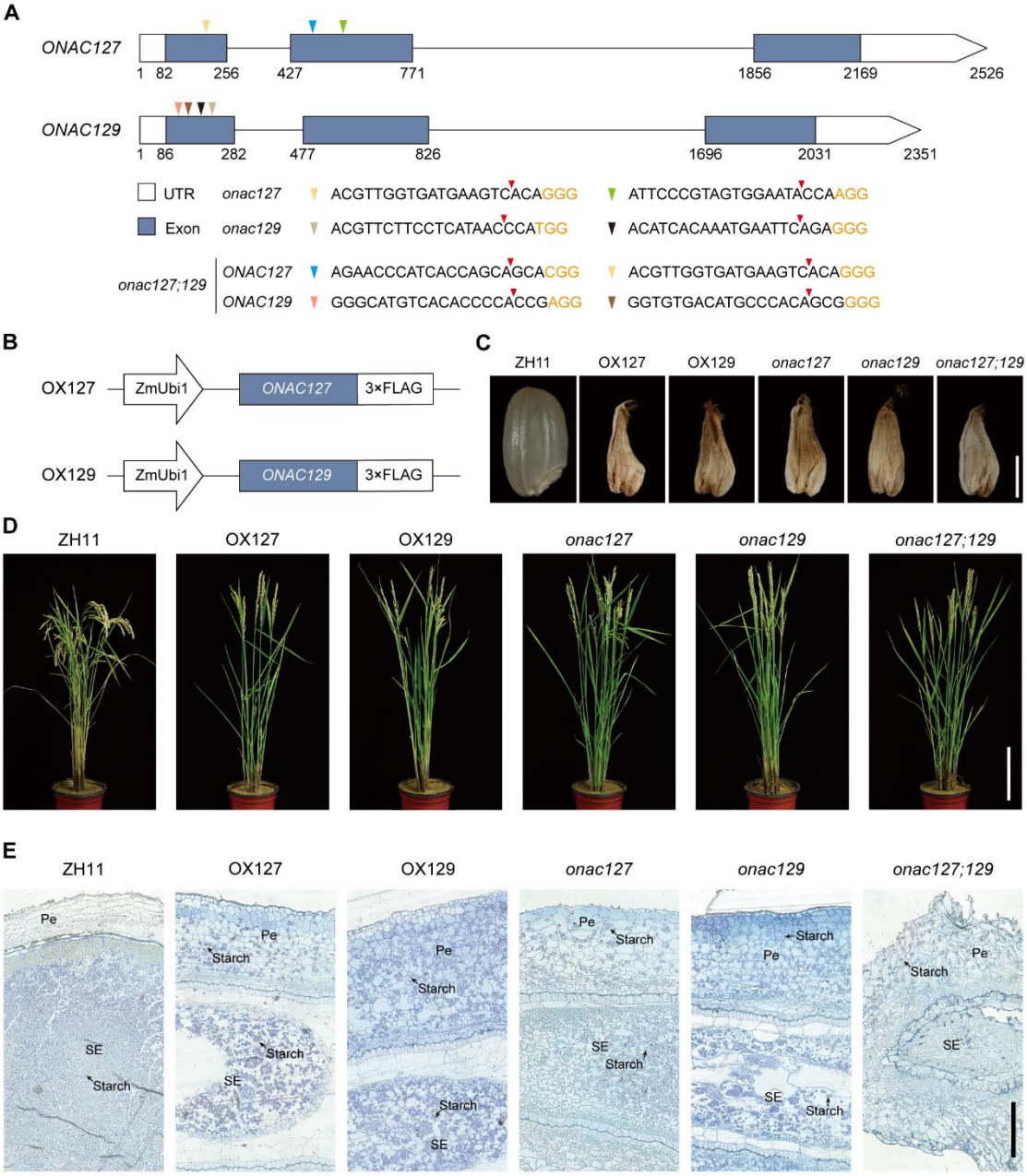

Fig. 3 The construction of the CRISPR mutants and overexpression plants and their phenotypes. A. Schematic diagram of the sgRNA target site in genomic region of *ONAC127* and *ONAC129*. The target sequences of *onac127*, *onac129* and *onac127;129* are listed under the diagram and marked as a colorful triangle. The Cas9 splice sites are marked as red triangle and the protospacer-adjacent motifs are shown in orange. B. Schematic diagram of the construction of OX127 & OX129. C. Phenotypes of grains of the overexpression lines and mutants of *ONAC127* and *ONAC129*. Scale bars are 2 mm. D. Phenotypes of panicles at maturation stage. The panicles of transgenic plants are almost upright while

253 the panicles of ZH11 are bent due to the grain filling. Scale bars are 20 cm. E. Accumulation of starch
254 in the pericarp of the caryopsis of overexpression lines and mutants relative to ZH11. Cross sections of
255 caryopses stained with toluidine blue at 7DAP. Pe, pericarp; SE, starchy endosperm. Scale bar is 40
256 μm.

257 **ONAC127 and ONAC129 are involved in heat stress response**

258 With the measurement of agronomic traits, the transgenic lines of *ONAC127* and
259 *ONAC129* showed significant reduction in both seed set rate (percentage of fully filled
260 seeds after harvest) and 1000-grains weight (Fig. 4A, B). The percentage of shrunken
261 grains showed an obvious increase while proportion of blighted grains (glumes with no
262 seed in it) did not change significantly in these transgenic lines (Fig. 4C). It proved that
263 the reduction of seed set rate and yield was mainly caused by the increase of shrunken
264 grains.

265 Notably, the transgenic plants during filling stages were suffered from severe heat
266 stress in the summer of 2018 (Fig. 4D, E). Previous studies have shown that the ambient
267 temperature higher than 35℃ would have a serious impact on the yield at flowering
268 and grain filling stages (Hakata et al., 2017). Therefore, we set 35℃ as the heat damage
269 temperature of rice (T_B), and calculated the heat damage accumulated temperature per
270 hour (TH_i), heat damage accumulated temperature during filling stage (T_S) and heat
271 damage hours during filling stage (H_S) as described by Chen (Chen et al., 2019). Given
272 that *ONAC127* and *ONAC129* function during early filling stage, we also calculated the
273 heat damage accumulated temperature during 0-7 DAP (T_{S7}) and heat damage hours
274 during 0-7 DAP (H_{S7}). Noting that we cultivated two batches of rice in the summer of
275 2018, the first batch of plants were flowering on about July 20 when the second batch
276 goes on about August 20. It's obvious that T_S and H_S of the first batch were much higher
277 than that of the second batch, especially at the early development stage of caryopsis
278 (Fig. 4D, E).Therefore, the caryopses of the plants cultivated in the first batch were
279 defined as suffering from heat stress while those in the second batch were defined as

planted under normal conditions with little or no heat stress. We found that heat stress caused sharp increase of shrunken grains compared to normal conditions, and such increase in *onac127;129* was more dramatic than the other transgenic lines (Fig. 4C), which led to significant decrease of seed set rate and 1000-grains weight (Fig. 4A, B). Meanwhile, the expression level of *ONAC127* and *ONAC129* was highly increased under heat stress (Supplemental Fig. S6), which suggested that *ONAC127* and *ONAC129* might be involved in heat stress response during caryopsis filling stage.

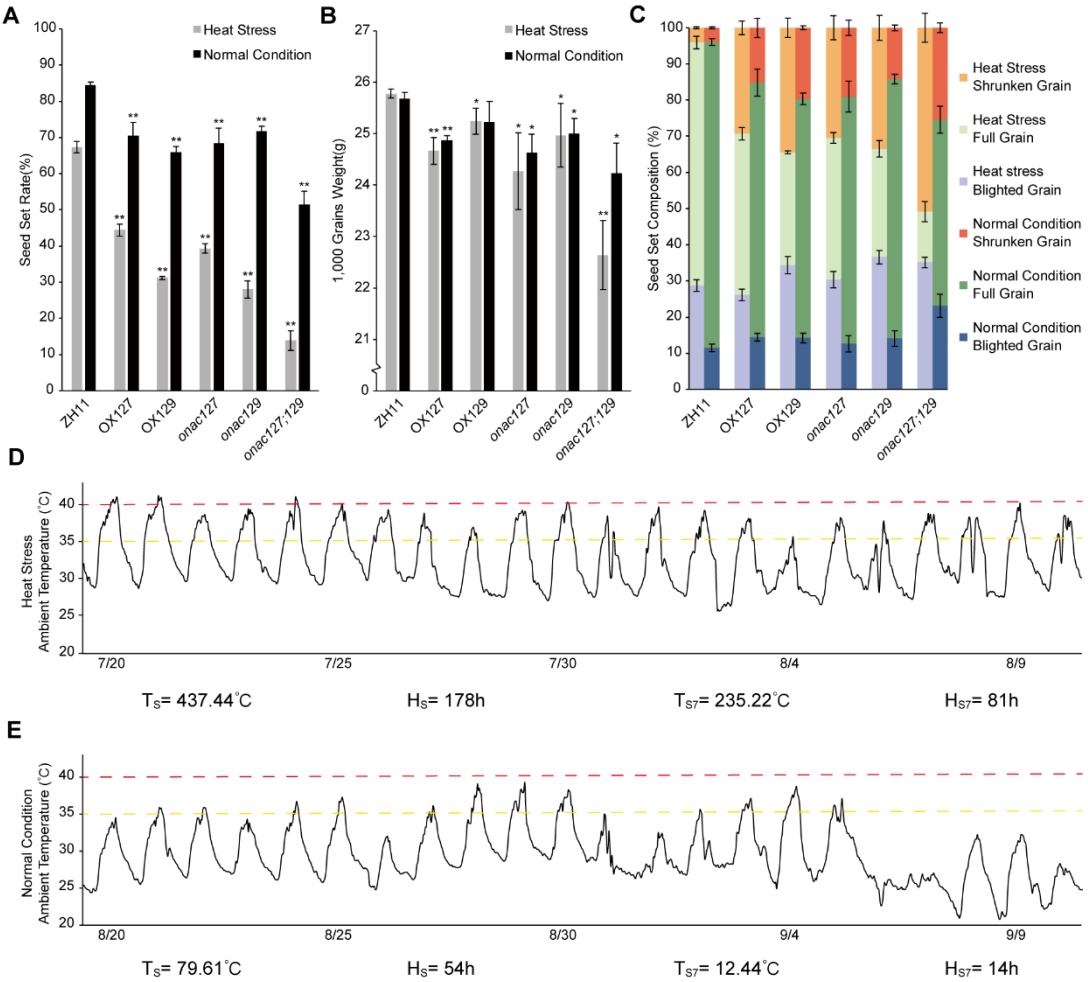

Fig. 4 Agronomic traits analyses and ambient temperature.

A. Seed set rate. The ratio of full grains to all spikelets on a panicle. B. 1,000 grains weight. Only the fully filled grains were counted and the data was calculated based on 100 grains. C. The composition of the seed set of spikelets. Data in (A), (B) and (C) are meant (±SD) from three independent lines, each of which are meant from three biological replicates. Significant differences between the ZH11 and the

293 transgenic lines were determined using Student's t-test (* P<0.05, ** P<0.01). D and E. The ambient
294 temperature of growing areas during rice caryopsis filling stage. 35°C is marked as yellow dotted lines
295 and 40°C is marked as red dotted lines. T_S, heat damage accumulated temperature during whole filling
296 stage; H_S, heat damage hours during whole filling stage; T_{S7}, heat damage accumulated temperature
297 during 0-7 DAP; H_{S7}, heat damage hours during 0-7 DAP.

298 **ONAC129 negatively regulates ONAC127 transcriptional activity**

299 For deeper exploring the relationship of *ONAC127* and *ONAC129*, we performed
300 a dual luciferase assay in rice protoplasts as the transcriptional activity of the two genes
301 was not detected in yeast assays (Fig. 2A). *ONAC127* and *ONAC129* were fused with
302 the yeast GAL4 binding domain (GAL4BD) as effectors to be co-transformed into rice
303 protoplasts with a firefly luciferase reporter gene driven by a CaMV35S promotor (35S-
304 GAL4-fLUC; Fig. 5A). A significant increase in the transcriptional activation activity
305 of ONAC127 and ONAC129 was detected, while the transcriptional activity of
306 ONAC127 was significantly restrained when ONAC129 was co-transformed into rice
307 protoplasts (Fig. 5B). These results hinted that ONAC129 might regulate the
308 transcriptional activity of ONAC127 negatively and we wonder if ONAC129 could
309 regulate the expression of *ONAC127*. However, we didn't find significant fluctuation
310 of the expression of *ONAC127* in the transgenic lines of *ONAC129* and vice versa.
311 (Supplemental Fig. S6).

312 As we know, several NAC transcription factors contain both transcriptional
313 activation domain and NAC repression domain (NARD), which means that the
314 combinatorial effects of both transcriptional regulation activities determine
315 downstream events (Hao et al., 2010). Hence, we decided to BLAST and analyze the
316 protein sequences of ONAC127 and ONAC129 through the method described by Hao,
317 and we found that there were NARD-like sequences in NAC subdomain D indeed in
318 both genes (Fig. 5C), which suggested that *ONAC127* and *ONAC129* might be
319 bifunctional transcription factors that could activate or repress downstream genes in

320 different situation.

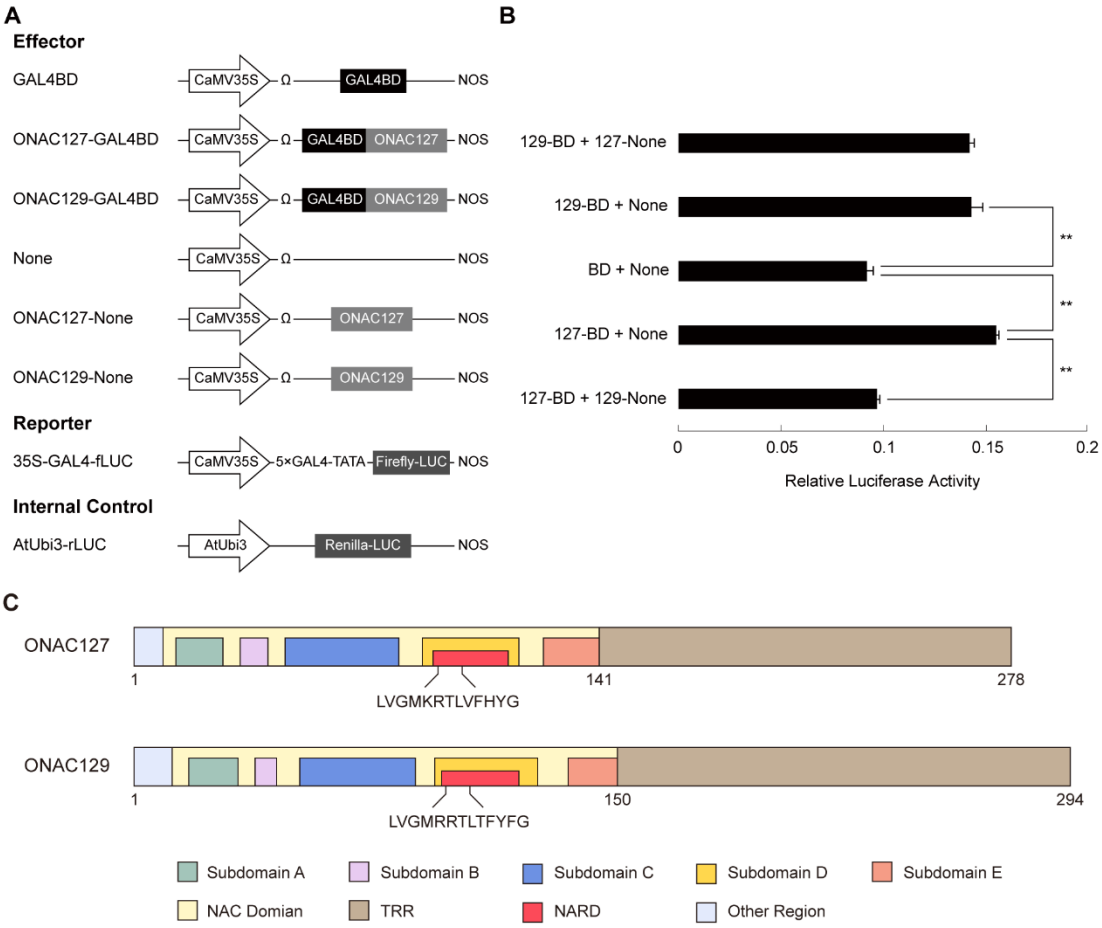

321

322 **Fig. 5 ONAC129 negatively regulates ONAC127 transcriptional activity.**

323 A. Scheme of the constructs used in the rice protoplast cotransfection assay. B. Data of Dual-LUC
324 assay. The reporter and internal control are co-transformed with each experimental group. The
325 fLUC/rLUC ratio represents the relative activity of CaMV35S promoter. The values in each column are
326 the mean (±SD) of three replicates. Significant differences are determined using Student's t-test (**
327 P<0.01). C. Schematic diagram of the domains of ONAC127 & ONAC129. The color legends
328 indicating the domains are shown at the bottom of the figure.

329 ONAC127 and ONAC129 regulate the transcription of genes related to sugar 330 transportation and abiotic stimulus

331 RNA-Seq analyses worked in identifying differentially expressed genes. The 7
332 DAP caryopses of the overexpression lines and mutants of *ONAC127* and *ONAC129*
333 under heat stress and normal conditions were used to generate RNA-seq libraries. There

334 are 7056, 6485, 5765, and 1608 differentially expressed genes (DEGHs) identified in
335 *onac127* (*onac127*H), *onac129* (*onac129*H), OX127 (OX127H), OX129 (OX129H)
336 respectively under heat stress, compared with ZH11 (ZH11H), and 15334, 13284, 1776,
337 2041 differentially expressed genes (DEGNs) which were identified in *onac127*
338 (*onac127*N), *onac129* (*onac129*N), OX127 (OX127N), OX129 (OX129N) respectively
339 under normal conditions compared with ZH11 (ZH11N) (Fig. 6A, B; Supplemental
340 Dataset S1). Gene Ontology (GO) enrichment analyses was performed to examine the
341 biological roles of DEGs in caryopsis development. The significantly enriched GO
342 terms were mainly associated with stimulus response, transcriptional activity regulation,
343 signal transduction, cell wall construction and substance transportation (Fig. 6C).
344 Subsequently, the genes directly bound by ONAC127 and ONAC129 in caryopsis
345 were identified using Chromatin Immunoprecipitation Sequencing assays (ChIP-seq).
346 The ChIP assays were performed using the anti-FLAG antibody with 7 DAP caryopses
347 of OX127 (OX127H), OX129 (OX129H) under heat stress, and OX127 (OX127N),
348 OX129 (OX129N) under normal condition. The expression of the ONAC127-FLAG
349 and ONAC129-FLAG fusion proteins was verified by western blot analyses to validate
350 the effectiveness of the FLAG tags (Supplemental Fig. S7). After sequencing, 185, 6125,
351 220, 455 peaks were finally obtained respectively in OX127H, OX127N, OX129H and
352 OX129N (Supplemental Dataset S2), and 54, 5092, 82, 212 putative ONAC127 and
353 ONAC129 bound genes were identified in OX127H, OX127N, OX129H and OX129N
354 respectively among the peaks (Fig. 6D). Then, we identified the binding motifs of the
355 ONACs using MEME (Machanick and Bailey, 2011), and found that the significantly
356 enriched motif was 'CT(C)TTCT(C)TT' (Fig. 6E, F), in line with 'TT(A/C/G)CTT',
357 the specific motif of transmembrane NAC transcription factors *NTL6* and *NTL8*
358 (Lindemose et al., 2014). Both the two genes were associated with stimulus response,
359 implying that *ONAC127* and *ONAC129* were probably involved in stress response.
360 Notably, the motif 'CT(C)TTCT(C)TT' was only found significantly in OX127H and
361 OX129H. There was no significantly enriched motif in OX127N and OX129N,

362 implying that the target genes of ONAC127 and ONAC129 might be more specific
363 under heat stress.

364 For further exploring the target genes regulated by ONAC127 and ONAC129, we
365 defined the genes which were either consistently bound by ONAC127/129 or
366 simultaneously bound by ONAC127 and ONAC129 under heat stress or normal
367 conditions as ONAC127/129 preferable-bound genes (Fig. 6D, red trapezoid). Based
368 on the data from RNA-Seq analyses and phenotype of transgenic lines of ONAC127
369 and ONAC129, 8 genes with respect to sugar transportation or abiotic stress response
370 were selected from 136 preferable-bound genes as the potential target genes (PTGs) of
371 ONAC127 and ONAC129 for further investigation.

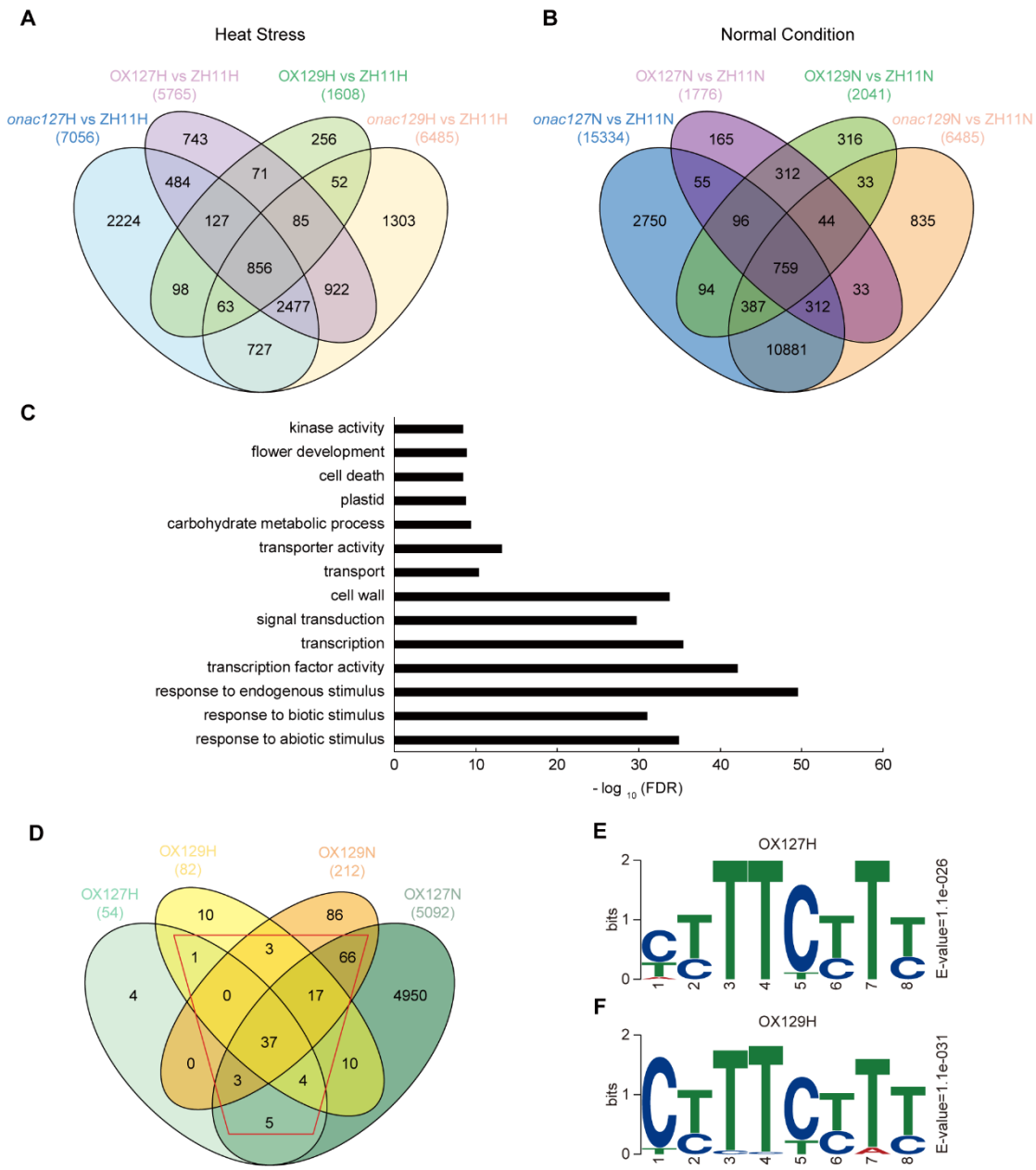

Fig. 6 Data analyses of RNA-Seq and ChIP-Seq.

A and B. Venn diagram showing the number of genes regulated by *ONAC127* and *ONAC129* based on the RNA-seq analyses. Differentially expressed genes are defined as |Fold Change|≥2 and *p*-value<0.05. *p*-values were calculated using the Fisher's exact test. C. A selection of enriched gene ontology (GO) terms of the differentially expressed genes. GO terms with FDR <0.05 were kept. The length of the bars represents the negative logarithm (base 10) of FDR. D. Venn diagram showing the number of ONAC127 and ONAC129 direct target genes. The red trapezoid indicates the ONAC127 and ONAC129 preferable bound genes. E and F. Motif analyses of ONAC127 and ONAC129 binding

381 peaks. The E-value is the enrichment P-value multiplied by the number of candidate motifs tested.

382 **ONAC127 and ONAC129 play a pivotal role in caryopsis filling through**
383 **regulating key factors directly in substance accumulation and stress response**

384 To validate the interactions between ONAC127/129 and promotors of their
385 potential target genes (PTGs), the yeast one-hybrid assays were performed. It suggested
386 that ONAC127 and ONAC129 could bind to the promoter sequences of *OsEATB*,
387 *OsHCI1*, *OsMSR2*, *OsSWEET4*, *bHLH144* and *OsMST6* directly in yeast (Fig. 7A). The
388 Dual-LUC assays in rice protoplasts were performed to figure out whether ONAC127
389 and ONAC129 affect the transcription of these genes directly. ONAC127 and
390 ONAC129 were co-transformed into rice protoplasts with a firefly luciferase reporter
391 gene driven by target gene promotors (Fig. 7B). It turned out that ONAC127 activated
392 *OsMSR2* and *OsMST6* promotors significantly, and both ONAC127 and ONAC129
393 repressed the *OsEATB* and *OsSWEET4* promotors strongly *in vivo*. It is noteworthy that
394 ONAC129 could suppress the transcriptional activation activity of ONAC127 to
395 *OsMSR2* and *OsMST6* promotors, while ONAC129 barely regulated the transcription
396 of *OsMSR2* and *OsMST6* alone (Fig. 7C).

397 For testing whether the endogenous ONAC127 and ONAC129 bound to the target
398 genes specifically, ChIP-qPCR was performed using the same rice materials of ChIP-
399 Seq. The result indicated that ONAC127 and ONAC129 bound to the promoters of
400 *OsEATB*, *OsMSR2*, *OsSWEET4* and *OsMST6* respectively under heat stress and normal
401 conditions (Fig. 7D, E, F, G). The qRT-PCR for these genes was also performed in the
402 7 DAP caryopses of transgenic lines of *ONAC127* and *ONAC129*, showing that the
403 expression of *OsEATB* and *OsSWEET4* was significantly up-regulated in the mutants
404 and generally down-regulated in the overexpression lines. The expression of *OsMSR2*
405 and *OsMST6* was both up-regulated in *onac129* and down-regulated in *onac127*
406 (Supplemental Fig. S8). The results above indicated that *OsEATB*, *OsMSR2*,
407 *OsSWEET4* and *OsMST6* were the direct targets of ONAC127 and ONAC129 in rice

408 during caryopsis filling.

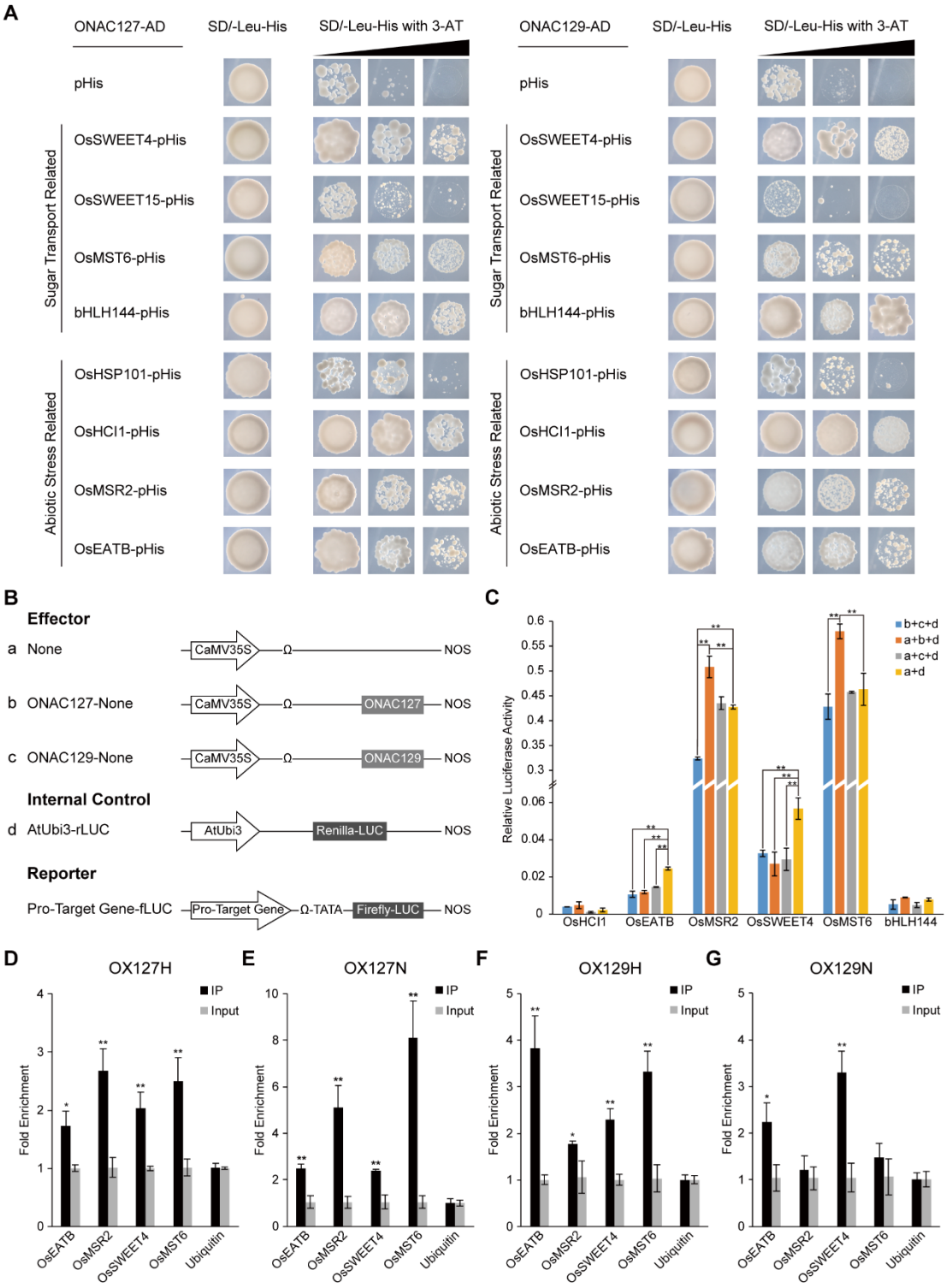

409

410 **Fig. 7 Identification and validation of ONAC127 and ONAC129 direct target genes in rice.**

411 A. The interaction between ONAC127/129 and the promoters of PTGs as determined by yeast one-

412 hybrid analyses. The transformants were grown on [SD/–Leu /–His] plates with 3-AT which

413 concentrations were 50mM, 100mM and 150mM respectively. B. Scheme of the constructs used in the

414 rice protoplast cotransfection assay. C. Data of Dual-LUC assay. The fLUC/rLUC ratio represents the
415 relative activity of target gene promoters. D-G. ChIP-qPCR verification of ONAC127 and ONAC129
416 binding regions. The values in each column are the mean (±SD) of three replicates. Significant
417 differences were determined using Student's t-test (* P<0.05; ** P<0.01).

418 **DISCUSSION**

419 In this study, two rice caryopsis-specific NAC transcription factors *ONAC127* and
420 *ONAC129* were identified, which can form a heterodimer and are predominantly
421 expressed during the early and middle stage of rice caryopsis development (Fig. 1, 2).
422 The caryopses of the transgenic plants were obviously unfilled (Fig. 3C, D, E;
423 Supplemental Fig. S5), and the proportion of shrunken grains was higher under natural
424 heat stress (Fig. 4C). By protein−DNA binding assays, we found that ONAC127 and
425 ONAC129 may regulate the expression of the sugar transporters, *OsMST6* and
426 *OsSWEET4* directly. Both the two genes are involved in the transportation of
427 photosynthate from dorsal vascular bundles to endosperm during caryopsis filling
428 (Wang et al., 2008; Sosso et al., 2015). ONAC127 and ONAC129 also bind to the
429 promotors of *OsMSR2* and *OsEATB* directly (Fig. 7), which participate in abiotic stress
430 responses by responding to calcium ion (Ca^{2+}) or plant hormones (Qi et al., 2011; Xu
431 et al., 2011). These findings suggest that *ONAC127* and *ONAC129* may be involved in
432 multiple pathways, therefore interfere the abiotic stress response and caryopsis filling
433 process during rice reproductive stage.

434 **ONAC127 and ONAC129 are involved in the apoplasmic transportation of**
435 **photosynthates as a balancer**

436 At the early stage of caryopsis development, some of the photosynthate from the
437 dorsal vascular bundle was transported to endosperm through the apoplasmic space
438 formed by degenerative nucellar cell wall, the others synthesized the starch grains in
439 mesocarp cells (Hoshikawa, 1984). The starch accumulation in pericarp will reach a

440 maximum at 5 DAP. After that, the starch in mesocarp cells will be disintegrated and
441 the nutrient will be transported to the endosperm due to the continuous process of
442 endosperm cells filling. The cell contents of pericarp cells will disappear, and the cells
443 will eventually dehydrate and die, leaving only the cuticularized cell wall remnants (Wu
444 et al., 2016).

445 Since the abnormal expression of *ONAC127* and *ONAC129*, endosperm cells in
446 abnormal caryopses may not obtain enough photosynthate for filling due to the
447 functional defect of apoplasmic transport pathways. The photosynthates accumulates in
448 pericarp as starch grains without been disintegrated, thus stop the endosperm cells from
449 proliferation or filling by starch, eventually leading to incompletely filled and shrunken
450 caryopsis (Fig. 3C, E).

451 It is noteworthy that the target transporters *OsSWEET4* and *OsMST6* are
452 predominantly expressed at early stages of caryopsis development, and may act in
453 downstream of the cell wall invertase OsCIN2 to import hexose into aleurone layer
454 through apoplasmic space (Wang et al., 2008; Sosso et al., 2015; Yang et al., 2018). As
455 previously mentioned, ONAC127 and ONAC129 suppress the expression of
456 *OsSWEET4* directly (Fig. 7C; Supplemental Fig. S8), and *ossweet4-1*, the mutant of
457 *OsSWEET4*, has a distinct phenotype with shrunken grains similar with the abnormal
458 caryopses in transgenic lines of *ONAC127* and *ONAC129* (Sosso et al., 2015). The fact
459 confirmed our hypothesis that *ONAC127* and *ONAC129* are involved in the apoplasmic
460 transport pathways directly by regulating the expression of transporters indeed.

461 Moreover, the shrunken caryopses we observed in mutants and overexpression
462 lines of *ONAC127* and *ONAC129* are also similar with the incompletely filled
463 caryopses of the double mutants *ossweet11;15*, in which two apoplasmic transporters
464 OsSWEET11 and OsSWEET15 were dysfunction (Yang et al., 2018). For that
465 *OsSWEET15* has been excluded from the target genes by the yeast one-hybrid assays
466 (Fig. 7A), we detected the expression of *OsSWEET11* and *OsSWEET15* in transgenic
467 lines of *ONAC127* and *ONAC129* by qRT-PCR and found that both genes might be

468 activated by ONAC127 and ONAC129 indirectly (Supplemental Fig. S9). The fact
469 suggested that ONAC127 and ONAC129 might activate the expression of
470 *OsSWEET11/15* and suppress the expression of *OsSWEET4* simultaneously. This may
471 explain the fact that the phenotypes of mutants and overexpression lines of *ONAC127*
472 and *ONAC129* are almost the same in incompletely filled caryopses (Fig. 3C, D, E;
473 Supplemental Fig. S5). Hence, we speculate that *ONAC127* and *ONAC129* may act as
474 a balancer in apoplasmic transportation by activating or suppressing the expression of
475 transporters dynamically (Fig. 8), therefore keeping the amount of several different
476 apoplasmic transporters at different stages of caryopsis development.

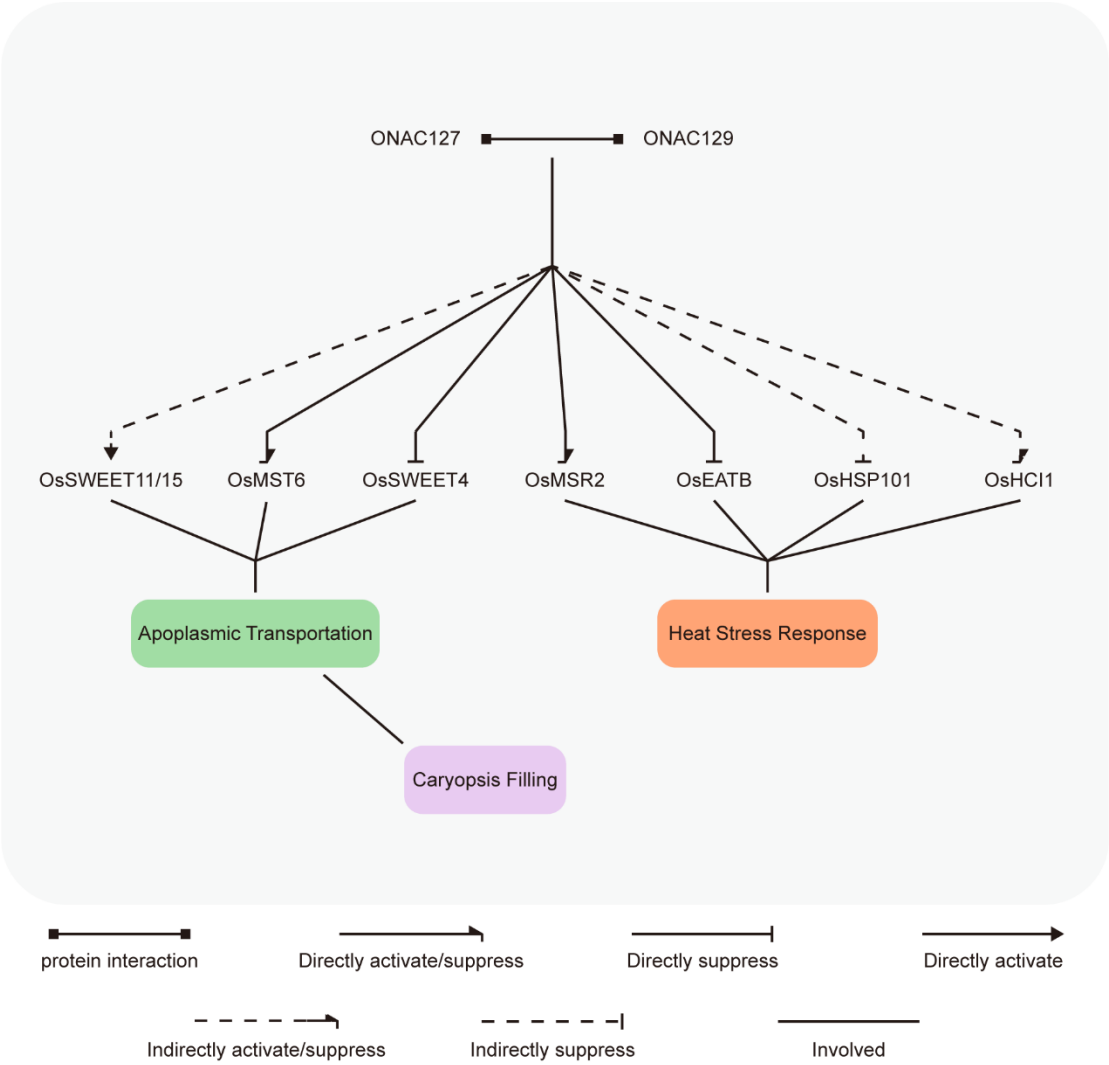

477

478 **Fig. 8 Schematic diagram of the working model of ONAC127 and ONAC129 in rice caryopsis.**

479 ONAC127 and ONAC129 regulate the expression of *OsMST6* and *OsSWEET4* directly to participate in
480 the apoplasmic transportation, and OsSWEET11 and OsSWEET15 may be also involved in this
481 process as the indirect downstream transporters of them. When heat stress occurs, ONAC127 and
482 ONAC129 may be involved in the response to heat stress during the filling stage by regulating the
483 expression of *OsMSR2* and *OsEATB* directly, while *OsHCI1* and *OsHSP101* are regulated indirectly.
484 ONAC127 and ONAC129 may act as the balancer of apoplasmic transportation and the core
485 transcription factors in the stress response during the early and middle stages of rice caryopsis
486 development.

487 ONAC129 suppresses the transcriptional activity of ONAC127 in some pathways,
488 meanwhile, ONAC127 and ONAC129 may regulate downstream genes differently at
489 dimer state and monomer state (Fig. 5B, 7C). We conjecture that the proportion of
490 ONAC127/129 dimers may be vital in adjusting the balance of the amount of
491 apoplasmic transporters at different stages of caryopsis development. Whether to
492 knockout or to over-express *ONAC127* or *ONAC129*, the proportion of the monomers
493 and dimers of ONAC127/129 will be changed inevitably, which induces various
494 changes in expression of the apoplasmic transporters, thus the apoplasmic
495 transportation defects, leading to the incomplete filling caryopsis phenotype (Fig. 3C).
496 In macroscopic view, the balance regulation of apoplasmic transportation may be a
497 "rate-limiting step" of rice reproductive growth to ensure that the photosynthate is
498 enough for both the filling of grains and the energy for plants to avoid premature aging,
499 thus may be vital for plants to keep the balance of vegetative growth and reproductive
500 growth.

501 **ONAC127 and ONAC129 respond to heat stress during caryopsis filling**

502 Heat stress has profound effects on plant growth, particularly in reproductive
503 development. When plants encounter heat stress, the rise of cytosolic Ca^{2+}
504 concentration is the most rapid response (Liu et al., 2003). With the increase of Ca^{2+}
505 concentration, the expression of calmodulins (CaMs) and Calmodulin-like genes

506 (CMLs) will be activated and modulate the phosphorylation state of HSFs to regulate
507 their DNA binding ability, thereby regulating the expression of heat stress related genes
508 including HSPs and some plant hormone responsive genes (Li et al., 2018).

509 The proportion of incompletely filled caryopses under heat stress is much higher
510 than that of normal condition (Fig. 4C), and the expression of *ONAC127* and *ONAC129*
511 was induced by heat stress (Supplemental Fig. S6), suggesting that heat stress might
512 interfere the dimerization of ONAC127 and ONAC129 to affect the balance of
513 apoplastic transportation. As previously mentioned, ONAC127 and ONAC129 regulate
514 the expression of *OsMSR2* and *OsEATB* directly (Fig. 6C; Supplemental Fig. S8).
515 Previous study showed that *OsMSR2*, which can be strongly induced by heat, cold and
516 drought stress, is a calmodulin-like protein working by binding Ca^{2+} and speculated
517 having the function as a Ca^{2+} sensor in plant cells (Xu et al., 2011). *OsEATB* is a rice
518 AP2/ERF gene which can suppress gibberellic acid (GA) synthesis while the GA
519 signaling pathway involved in the regulation of cell elongation and morphogenesis
520 under heat stress (Koini et al., 2009; Qi et al., 2011). We hereby speculated that
521 *ONAC127* and *ONAC129* might participate in heat stress response by regulating the
522 Ca^{2+} and GA signaling pathway.

523 The expression level of *OsHSP101* and *OsHCI1* was changed significantly in the
524 transgenic lines of *ONAC127* and *ONAC129* (Fig. 7A, C; Supplemental Fig. S9). We
525 believe that they are also the potential target genes of ONAC127 and ONAC129, though
526 they may not be regulated directly. RING E3 ligase gene *OsHCI1* is induced by heat
527 stress and mediates nuclear–cytoplasmic trafficking of nuclear substrate proteins via
528 mono-ubiquitination to improve the heat tolerance under heat shock (Lim et al., 2013).
529 Meanwhile, OsHSP101 function as one of the important molecular chaperones that
530 interact with OsHSA32 and OsHsfA2c, the latter of which is one of the central
531 regulators of heat stress response (Singh et al., 2012; Lin et al., 2014). Accordingly, we
532 believe that *ONAC127* and *ONAC129* are involved in some core reactions in the heat
533 stress response during rice caryopsis development stage.

534 Ca^{2+} is one of the most important second messengers in heat stress response,
535 cytosolic Ca^{2+} concentration would change rapidly in a short time when heat stress
536 occurs (Li et al., 2018). The stress signal would be then transmitted by CaMs/CMLs
537 like OsMSR2 to influence downstream gene expression consequently. When the
538 downstream HSFs are activated, HSPs including OsHSP101 would be induced to
539 express and function, and some nuclear-cytoplasmic trafficking reactions involving
540 OsHCI1 would occur (Singh et al., 2012; Lim et al., 2013). Besides, a variety of plant
541 hormones including GA would act in heat stress response to maintain plant growth, and
542 *OsEATB* plays an important role in GA-mediated plant cell elongation (Qi et al., 2011;
543 Li et al., 2018). Considering that all these direct or indirect target genes of *ONAC127*
544 and *ONAC129* play vital roles in the key steps of the heat stress response regulatory
545 network, we speculate that ONAC127 and ONAC129 may be the core transcription
546 factors in heat stress response during rice caryopsis filling stage, and the stress and
547 hormone response may be involved in the complex regulatory network of apoplasmic
548 transportation.

549 **MATERIALS AND METHODS**

550 **Generation of transgenic plants and growth conditions**

551 For generating CRISPR mutants, we used the web-based tool CRISPR-P v2.0
552 (http://cbi.hzau.edu.cn/CRISPR2/) designed by Liu (Liu et al., 2017) to get the specific
553 gRNA cassettes targeting *ONAC127* and *ONAC129* and then cloned into a binary vector
554 pYLCRISPR/Cas9-MH (Ma et al., 2015). For overexpression plants, we amplified the
555 stop-code-less cDNA fragments of *ONAC127* and *ONAC129*, fused 3×Flag or EGFP
556 coding sequence at the 3' end. The fused sequences were cloned into the binary vector
557 pCAMBIA1301U (driven by a maize ubiquitin promotor). For tissue specific
558 expression analyses, a 2000bp fragment of the 5' upstream region of *ONAC127*, and a
559 2043bp fragment of the 5' upstream region of *ONAC129* were cloned into the binary
560 vector pDX2181G (with GUS, β-glucuronidase).These recombinant constructs were

561 introduced into rice Zhonghua11 (ZH11; *Oryza sativa* ssp. *japonica)* by *Agrobacterium*
562 *tumefaciens* (EH105)-mediated transformation (Lin and Zhang, 2005). The plant
563 materials were cultivated in paddy fields in Huazhong Agricultural University, Wuhan,
564 China, under natural long-day conditions (approximately 12-14 h light/10-12 h dark)
565 during May to October 2018. The temperature of growing areas during rice
566 reproductive stage was showed in (Fig. 4D, E). We set 35℃ as the heat damage
567 temperature of rice (T_B), and calculated the heat damage accumulated temperature per
568 hour (TH_i), $TH_i = \begin{cases} T_i - T_B & T_i \geq T_B \\ 0 & T_i < T_B \end{cases}$ (T_i is the ambient temperature at *i* hour); heat
569 damage hours during filling stage (H_S) , $H_s = \sum_{i=0}^{n} H_i$ ($H_i = \begin{cases} 1 & T_i \geq T_B \\ 0 & T_i < T_B \end{cases}$) and
570 heat damage accumulated temperature during filling stage (T_S), $T_S = \sum_{i=0}^{n} TH_i$ using
571 the method described by Chen (Chen et al., 2019). The heat damage accumulated
572 temperature during 0-7 DAP (T_{S7}) and heat damage hours during 0-7 DAP (H_{S7}) was
573 also calculated as the method above. The phenotypes were detected in homozygous T_1
574 generation of transgenic plants. The primer sequences used in this study were listed in
575 Supplemental Table S1 and would not be repeated in the following article.

576 **Histochemical GUS staining**

577 Unripe caryopses at 5 and 7 DAP from pONAC127::GUS and pONAC129::GUS
578 transgenic plants were collected for the GUS staining assays following the methods
579 described by Yang (Yang et al., 2018).

580 **Microscopy analyses**

581 For semithin section microscopy analyses, the unripe caryopses at 7 DAP were
582 collected in 2.5% glutaraldehyde for fixation, vacuum infiltrated on ice for 30 min and
583 incubated at 4℃ for 24h. The plastic embedding and sectioning were performed as
584 described by Wang (Wang et al., 2008). Slides were stained with toluidine blue and
585 detected by a BX53 microscope (Olympus).

586 **RNA *in situ* hybridization**

587 Unripe caryopses (1-10 DAP) from rice ZH11 were collected for paraffin
588 embedding. Paraffin section was performed according to the previous method (Xiong
589 et al., 2019). Gene-specific fragments of *ONAC127* and *ONAC129* were amplified by
590 the primers used in RT-PCR and cloned into the pGM-T vector. The probes were
591 synthesized using the DIG RNA labeling kit (SP6/T7) (Roche) according to the
592 manufacturer's recommendations. RNA hybridization and immunologic detection of
593 the hybridized probes were performed on sections as described by Kouchi (Kouchi and
594 Hata, 1993). Slides were observed using a BX53 microscope (Olympus).

595 **Transient expression assays**

596 To investigate the subcellular localization of ONAC127 and ONAC129, the CDS
597 of these genes were cloned into the pM999-35S vector, the nuclear located gene *Ghd7*
598 was used as a nuclear localization marker (Xue et al., 2008).For the BiFC assays, the
599 CDS of *ONAC127* and *ONAC129* were cloned into the vectors pVYNE and pVYCE
600 (Waadt et al., 2008) respectively. Plasmids were extracted and purified using the
601 Plasmid Midi Kit (QIAGEN) and were then transformed into rice protoplasts according
602 to the procedure described by Shen (Shen et al., 2017). The fluorescent signals were
603 detected with a confocal laser scanning microscope (TCS SP8, Leica).

604 **RNA isolation and transcript analyses**

605 Total RNA was isolated using the TRIzol method (Invitrogen), and the first strand
606 cDNA was synthesized using HiScript II Reverse Transcriptase (Vazyme). The real-
607 time PCR was performed on QuantStudio 7 Flex Real-Time PCR System (Applied
608 Biosystems), with the $2^{-\Delta\Delta Ct}$ method for relative quantification (Livak and Schmittgen,
609 2001). The significance of differences was estimated using Student's t-test. Relevant
610 primers were designed according to qPrimerDB (https://biodb.swu.edu.cn/qprimerdb)
611 (Lu et al., 2018).

612 **Yeast assays**

613 For yeast two-hybrid assay, the CDS of *ONAC127* and *ONAC129* were cloned into
614 the pGBKT7 and pGADT7 vector (Clontech). The fusion plasmids were transformed
615 into yeast strain AH109 or Y187. The pGBKT7-53 was co-transformed with pGADT7-
616 T as a positive control. For yeast one-hybrid assay, DNA fragments about 1000bp
617 corresponding to the promoters of target genes were independently inserted into the
618 pHisi-1 plasmid (Clontech). *ONAC127* and *ONAC129* were fused to GAL4
619 transcriptional activation domain (pGAD424). These constructs were transformed into
620 the yeast strain YM4271. Yeast two-hybrid assay and one-hybrid assay were performed
621 following the manufacturer's instructions (Clontech).

622 **Chromatin immunoprecipitation (ChIP)**

623 Overexpression lines of *ONAC127* and *ONAC129* (fused with 3×FLAG) were used
624 for ChIP-Seq analyses. We verified the expression of target proteins by western blot
625 using ANTI-FLAG M2 Monoclonal Antibody (Sigma-Aldrich). ChIP assay was
626 performed with ANTI-FLAG M2 Magnetic Beads (Sigma-Aldrich) as the method
627 described previously (Xiong et al., 2019). For each library, three independent replicated
628 samples were prepared. The immunoprecipitated DNA and input DNA were subjected
629 to being sequenced on the HiSeq 2000 platform (Illumina), which was processed by the
630 Novogene Corporation.

631 ChIP-Seq raw sequencing data was mapped to the rice reference genome (RGAP
632 ver. 7.0, http://rice.plantbiology.msu.edu) (Kawahara et al., 2013) using BWA (Li and
633 Durbin, 2009). MACS2 (Zhang et al., 2008) was used for peak calling and the peaks
634 were identified as significantly enriched (corrected P-value <0.05) in the IP libraries
635 compared with input DNA. Visual analyses were performed using IGV (Intergative
636 Genomics Viewer, v2.3.26) (Robinson et al., 2011). Motif enrichment analyses were
637 performed by MEME (Machanick and Bailey, 2011) with default parameters.

638 To validate the specific targets genes, the immunoprecipitated DNA and input DNA

639 was applied for ChIP-qPCR analyses. The enrichment value was normalized to the
640 input sample. The significance of differences was estimated using Student's t-test.

641 **RNA-Seq**

642 Total RNA was extracted from unripe caryopses at 7 DAP. For each library, three
643 independent replicated RNA samples were prepared. The RNA samples were then
644 sequenced on the HiSeq 2000 platform (Illumina), which was processed by the
645 Novogene Corporation.
646 The raw reads were filtered for adaptors and low-quality reads. Clean reads were
647 mapped to the reference genome of rice (RGAP v. 7.0) using HISAT2 (v.2.0.5) (Kim et
648 al., 2015). The gene expression level was calculated by FPKM method (Trapnell et al.,
649 2010), and the differentially expressed genes (|Fold Change| $\geq$ 2 and p-value<0.05)
650 were selected by DESeq2 software (Love et al., 2014). GOseq (Young et al., 2010) was
651 used for GO enrichment analyses, and p-value was converted to $-\log_{10}$(p-value) for
652 display.

653 ***In vitro* GST pull-down assay**

654 The CDS of *ONAC127* and *ONAC129* were cloned into pET28a and pGEX-4-1
655 vectors respectively for His-tagged ONAC127 and GST-tagged ONAC129 protein
656 expression *in vitro*. The fusion plasmids were transformed into *Escherichia coli* BL21
657 strain. The GST pull-down assays were performed according to the previous methods
658 (Xiong et al., 2019). The protein was separated on a 10% SDS-PAGE gel and further
659 analyzed by immunoblotting using anti-His and anti-GST antibody (Sigma-Aldrich).

660 **Dual Luciferase Transcriptional Activity Assay**

661 Full-length cDNAs of *ONAC127* and *ONAC129* were cloned to yeast GAL4
662 binding domain vectors (GAL4BD) and "None" as effectors. The 35S-GAL4-fLUC and
663 190-fLUC were used as reporters, and AtUbi::rLUC was used as an internal control.

664 The constructed plasmids were purified and transformed into rice protoplasts with the
665 procedure mentioned previously. Dual Luciferase Reporter Assay System (Promega)
666 was used to measure the luciferase activity by Tecan Infinite M200 (Tecan).

667 **Agronomic traits analyses**

668 Harvested ripe rice grains were air dried and stored at room temperature for at least
669 2 months before measuring. Only full grains were used for measuring 1000-grain
670 weight which was calculated based on 100 grains. The seed set rate/composition was
671 calculated based on the grains from 3-5 panicles (include the full, shrunken and blighted
672 grains). All measurements of the positive transgenic plants were undertaken using three
673 independent lines.

674 **Accession numbers**

675 The sequence data from this paper can be found in the RGAP database
676 (http://rice.plantbiology.msu.edu) under the following accession numbers: *ONAC025*
677 (LOC_Os11g31330), *ONAC127* (LOC_Os11g31340), *ONAC128* (LOC_Os11g31360),
678 *ONAC129* (LOC_Os11g31380), *OsMST6* (LOC_Os07g37320), *OsSWEET4*
679 (LOC_Os02g19820), *OsEATB* (LOC_Os09g28440), *OsMSR2* (LOC_Os01g72530),
680 *bHLH144* (LOC_Os04g35010), *OsHCI1* (LOC_Os10g30850), *HSP101*
681 (LOC_Os05g44340), *OsSWEET11* (LOC_Os08g42350), *OsSWEET15*
682 (LOC_Os02g30910), *OsbZIP63* (LOC_Os07g48820). The RNA-seq and ChIP-seq
683 data are deposited in the NCBI Gene Expression Omnibus (Edgar et al., 2002) with
684 accession number GSE140167.

685 **Supplemental Material**

686 **Supplemental Fig. S1** Expression level of mechanical isolation marker in isolated
687 tissue.

688 **Supplemental Fig. S2** Subcellular localization of the ONAC127 and ONAC129 in the

689 roots of two-week-old rice seedlings of pUbi::ONAC127-GFP and pUbi::ONAC129-
690 GFP transgenic plants.
691 **Supplemental Fig. S3** Mutation sites in *onac127*, *onac129* and *onac127;129* lines, as
692 compared with wild-type (ZH11) sequences.
693 **Supplemental Fig. S4** The relative expression level of the overexpression lines of
694 *ONAC127* and *ONAC129*.
695 **Supplemental Fig. S5** Different stages of caryopses development.
696 **Supplemental Fig. S6** Expression level of *ONAC127* and *ONAC129* in 7 DAP
697 caryopses of transgenic lines compared with that of ZH11.
698 **Supplemental Fig. S7** Detection of FLAG fusion proteins in the ZH11 and
699 overexpression lines.
700 **Supplemental Fig. S8** Expression level of the target genes of ONAC127 and
701 ONAC129 in 7 DAP caryopses of transgenic lines compared with that of ZH11.
702 **Supplemental Fig. S9** Expression level of the indirect target genes of ONAC127 and
703 ONAC129 in 7 DAP caryopses of transgenic lines compared with that of ZH11.
704 **Supplemental Table S1** Primers used in this study.
705 **Supplemental Dataset S1** Differentially expressed genes.
706 **Supplemental Dataset S2** Binding sites identified by ChIP-seq.

707 **ACKNOWLEDGEMENTS**

708 We thank Prof. Min Chen, Prof. Honghong Hu, Prof. Yidan Ouyang and Ms.
709 Wenjing Guo for helping revise the manuscript. This research was supported by grants
710 from the National Natural Science Foundation of China (no. 31570321). The funders
711 had no role in the study design, data collection and analysis, the decision to publish, or
712 in the preparation of the manuscript.

713 ## Author contributions

714 Y.R. and J.Y. conceived the original research plans; Y.R. carried out most of the
715 experiments; Z.H., Z.W., F.W. and Y.X. provided technical assistance to Y.R.; Y.R. and
716 H.J. analyzed the data; Y.R. conceived the project and wrote the article with
717 contributions of all the authors; J.Y. supervised and complemented the writing.

718 ## LITERATURE CITED

719 **Agarwal P, Kapoor S, Tyagi AK** (2011) Transcription factors regulating the progression of
720 monocot and dicot seed development. Bioessays **33:** 189-202
721 **Bai AN, Lu XD, Li DQ, Liu JX, Liu CM** (2016) NF-YB1-regulated expression of sucrose transporters
722 in aleurone facilitates sugar loading to rice endosperm. Cell Res **26:** 384-388
723 **Chen S, Zhang T, Huang Q, Chen M, Zhao L, Zhang Y** (2019) Effects of High Temperature Injury
724 on Seed Setting Rate from Heading to Milky Stage of Early Season Rice in Hainan. China
725 Tropical Agriculture**:** 65-69 (in Chinese with English abstract)
726 **Chen X, Lu S, Wang Y, Zhang X, Lv B, Luo L, Xi D, Shen J, Ma H, Ming F** (2015) OsNAC2 encoding
727 a NAC transcription factor that affects plant height through mediating the gibberellic acid
728 pathway in rice. Plant J **82:** 302-314
729 **Christianson JA, Dennis ES, Llewellyn DJ, Wilson IW** (2010) ATAF NAC transcription factors:
730 regulators of plant stress signaling. Plant Signal Behav **5:** 428-432
731 **Edgar R, Domrachev M, Lash AE** (2002) Gene Expression Omnibus: NCBI gene expression and
732 hybridization array data repository. Nucleic Acids Res **30:** 207-210
733 **Fang Y, Liao K, Du H, Xu Y, Song H, Li X, Xiong L** (2015) A stress-responsive NAC transcription
734 factor SNAC3 confers heat and drought tolerance through modulation of reactive oxygen
735 species in rice. J Exp Bot **66:** 6803-6817
736 **Fang Y, Xie K, Xiong L** (2014) Conserved miR164-targeted NAC genes negatively regulate
737 drought resistance in rice. J Exp Bot **65:** 2119-2135
738 **Fang Y, You J, Xie K, Xie W, Xiong L** (2008) Systematic sequence analysis and identification of
739 tissue-specific or stress-responsive genes of NAC transcription factor family in rice. Mol
740 Genet Genomics **280:** 547-563
741 **Fujita M, Fujita Y, Maruyama K, Seki M, Hiratsu K, Ohme-Takagi M, Tran LS, Yamaguchi-**
742 **Shinozaki K, Shinozaki K** (2004) A dehydration-induced NAC protein, RD26, is involved
743 in a novel ABA-dependent stress-signaling pathway. Plant J **39:** 863-876
744 **Hakata M, Wada H, Masumoto-Kubo C, Tanaka R, Sato H, Morita S** (2017) Development of a
745 new heat tolerance assay system for rice spikelet sterility. Plant Methods **13:** 34
746 **Hao YJ, Song QX, Chen HW, Zou HF, Wei W, Kang XS, Ma B, Zhang WK, Zhang JS, Chen SY**
747 (2010) Plant NAC-type transcription factor proteins contain a NARD domain for
748 repression of transcriptional activation. Planta **232:** 1033-1043
749 **Hoshikawa K** (1984) Development of Endosperm Tissue with Special Reference to the
750 Translocation of Reserve Substances in Cereals : III. Translocation pathways in rice

751 endosperm. Japanese journal of crop science **53:** 153-162
752 **Hu H, Dai M, Yao J, Xiao B, Li X, Zhang Q, Xiong L** (2006) Overexpressing a NAM, ATAF, and
753 CUC (NAC) transcription factor enhances drought resistance and salt tolerance in rice.
754 Proc Natl Acad Sci U S A **103:** 12987-12992
755 **Hu H, Xiong L** (2014) Genetic engineering and breeding of drought-resistant crops. Annu Rev
756 Plant Biol **65:** 715-741
757 **Huang D, Wang S, Zhang B, Shang-Guan K, Shi Y, Zhang D, Liu X, Wu K, Xu Z, Fu X, Zhou Y**
758 (2015) A Gibberellin-Mediated DELLA-NAC Signaling Cascade Regulates Cellulose
759 Synthesis in Rice. Plant Cell **27:** 1681-1696
760 **Ishimaru T, Ida M, Hirose S, Shimamura S, Masumura T, Nishizawa NK, Nakazono M, Kondo**
761 **M** (2015) Laser microdissection-based gene expression analysis in the aleurone layer and
762 starchy endosperm of developing rice caryopses in the early storage phase. Rice (N Y) **8:**
763 57
764 **Kawahara Y, de la Bastide M, Hamilton JP, Kanamori H, McCombie WR, Ouyang S, Schwartz**
765 **DC, Tanaka T, Wu J, Zhou S, Childs KL, Davidson RM, Lin H, Quesada-Ocampo L,**
766 **Vaillancourt B, Sakai H, Lee SS, Kim J, Numa H, Itoh T, Buell CR, Matsumoto T** (2013)
767 Improvement of the Oryza sativa Nipponbare reference genome using next generation
768 sequence and optical map data. Rice (N Y) **6:** 4
769 **Kim D, Langmead B, Salzberg SL** (2015) HISAT: a fast spliced aligner with low memory
770 requirements. Nat Methods **12:** 357-360
771 **Koini MA, Alvey L, Allen T, Tilley CA, Harberd NP, Whitelam GC, Franklin KA** (2009) High
772 temperature-mediated adaptations in plant architecture require the bHLH transcription
773 factor PIF4. Curr Biol **19:** 408-413
774 **Kouchi H, Hata S** (1993) Isolation and characterization of novel nodulin cDNAs representing genes
775 expressed at early stages of soybean nodule development. Mol Gen Genet **238:** 106-119
776 **Li B, Gao K, Ren H, Tang W** (2018) Molecular mechanisms governing plant responses to high
777 temperatures. J Integr Plant Biol **60:** 757-779
778 **Li H, Durbin R** (2009) Fast and accurate short read alignment with Burrows-Wheeler transform.
779 Bioinformatics **25:** 1754-1760
780 **Lim SD, Cho HY, Park YC, Ham DJ, Lee JK, Jang CS** (2013) The rice RING finger E3 ligase, OsHCI1,
781 drives nuclear export of multiple substrate proteins and its heterogeneous overexpression
782 enhances acquired thermotolerance. J Exp Bot **64:** 2899-2914
783 **Lin MY, Chai KH, Ko SS, Kuang LY, Lur HS, Charng YY** (2014) A positive feedback loop between
784 HEAT SHOCK PROTEIN101 and HEAT STRESS-ASSOCIATED 32-KD PROTEIN modulates
785 long-term acquired thermotolerance illustrating diverse heat stress responses in rice
786 varieties. Plant Physiol **164:** 2045-2053
787 **Lin YJ, Zhang Q** (2005) Optimising the tissue culture conditions for high efficiency transformation
788 of indica rice. Plant Cell Rep **23:** 540-547
789 **Lindemose S, Jensen MK, Van de Velde J, O'Shea C, Heyndrickx KS, Workman CT, Vandepoele**
790 **K, Skriver K, De Masi F** (2014) A DNA-binding-site landscape and regulatory network
791 analysis for NAC transcription factors in Arabidopsis thaliana. Nucleic Acids Res **42:** 7681-
792 7693

Liu H, Ding Y, Zhou Y, Jin W, Xie K, Chen LL (2017) CRISPR-P 2.0: An Improved CRISPR-Cas9 Tool for Genome Editing in Plants. Mol Plant **10:** 530-532

Liu HT, Li B, Shang ZL, Li XZ, Mu RL, Sun DY, Zhou RG (2003) Calmodulin is involved in heat shock signal transduction in wheat. Plant Physiol **132:** 1186-1195

Liu W, Xie X, Ma X, Li J, Chen J, Liu YG (2015) DSDecode: A Web-Based Tool for Decoding of Sequencing Chromatograms for Genotyping of Targeted Mutations. Mol Plant **8:** 1431-1433

Livak KJ, Schmittgen TD (2001) Analysis of relative gene expression data using real-time quantitative PCR and the 2(-Delta Delta C(T)) Method. Methods **25:** 402-408

Love MI, Huber W, Anders S (2014) Moderated estimation of fold change and dispersion for RNA-seq data with DESeq2. Genome Biology **15**

Lu K, Li T, He J, Chang W, Zhang R, Liu M, Yu M, Fan Y, Ma J, Sun W, Qu C, Liu L, Li N, Liang Y, Wang R, Qian W, Tang Z, Xu X, Lei B, Zhang K, Li J (2018) qPrimerDB: a thermodynamics-based gene-specific qPCR primer database for 147 organisms. Nucleic Acids Res **46:** D1229-D1236

Ma X, Zhang Q, Zhu Q, Liu W, Chen Y, Qiu R, Wang B, Yang Z, Li H, Lin Y, Xie Y, Shen R, Chen S, Wang Z, Chen Y, Guo J, Chen L, Zhao X, Dong Z, Liu YG (2015) A Robust CRISPR/Cas9 System for Convenient, High-Efficiency Multiplex Genome Editing in Monocot and Dicot Plants. Mol Plant **8:** 1274-1284

Machanick P, Bailey TL (2011) MEME-ChIP: motif analysis of large DNA datasets. Bioinformatics **27:** 1696-1697

Mao C, Ding W, Wu Y, Yu J, He X, Shou H, Wu P (2007) Overexpression of a NAC-domain protein promotes shoot branching in rice. New Phytol **176:** 288-298

Mathew IE, Das S, Mahto A, Agarwal P (2016) Three Rice NAC Transcription Factors Heteromerize and Are Associated with Seed Size. Front Plant Sci **7:** 1638

Matsuda T, Kawahara H, Chonan N (1979) Histo-Cytological Researches on Translocation and Ripening in Rice Ovary : I. Histological changes and transfer pathways in the developing ovary. Japanese journal of crop science **48:** 155-162

Nuruzzaman M, Manimekalai R, Sharoni AM, Satoh K, Kondoh H, Ooka H, Kikuchi S (2010) Genome-wide analysis of NAC transcription factor family in rice. Gene **465:** 30-44

Olsen AN, Ernst HA, Leggio LL, Skriver K (2005) DNA-binding specificity and molecular functions of NAC transcription factors. Plant Science **169:** 785-797

Ooka H, Satoh K, Doi K, Nagata T, Otomo Y, Murakami K, Matsubara K, Osato N, Kawai J, Carninci P, Hayashizaki Y, Suzuki K, Kojima K, Takahara Y, Yamamoto K, Kikuchi S (2003) Comprehensive analysis of NAC family genes in Oryza sativa and Arabidopsis thaliana. DNA Res **10:** 239-247

Oono Y, Wakasa Y, Hirose S, Yang L, Sakuta C, Takaiwa F (2010) Analysis of ER stress in developing rice endosperm accumulating beta-amyloid peptide. Plant Biotechnol J **8:** 691-718

Oparka KJ, Gates P (1981) Transport of assimilates in the developing caryopsis of rice (Oryza sativa L.) : The pathways of water and assimilated carbon. Planta **152:** 388-396

Patrick JW (1997) PHLOEM UNLOADING: Sieve Element Unloading and Post-Sieve Element

835 Transport. Annu Rev Plant Physiol Plant Mol Biol **48:** 191-222
836 **Qi W, Sun F, Wang Q, Chen M, Huang Y, Feng YQ, Luo X, Yang J** (2011) Rice ethylene-response
837 AP2/ERF factor OsEATB restricts internode elongation by down-regulating a gibberellin
838 biosynthetic gene. Plant Physiol **157:** 216-228
839 **Robinson JT, Thorvaldsdottir H, Winckler W, Guttman M, Lander ES, Getz G, Mesirov JP** (2011)
840 Integrative genomics viewer. Nat Biotechnol **29:** 24-26
841 **Schramm F, Larkindale J, Kiehlmann E, Ganguli A, Englich G, Vierling E, von Koskull-Doring P**
842 (2008) A cascade of transcription factor DREB2A and heat stress transcription factor HsfA3
843 regulates the heat stress response of Arabidopsis. Plant J **53:** 264-274
844 **Shen J, Liu J, Xie K, Xing F, Xiong F, Xiao J, Li X, Xiong L** (2017) Translational repression by a
845 miniature inverted-repeat transposable element in the 3' untranslated region. Nat
846 Commun **8:** 14651
847 **Shen J, Lv B, Luo L, He J, Mao C, Xi D, Ming F** (2017) The NAC-type transcription factor OsNAC2
848 regulates ABA-dependent genes and abiotic stress tolerance in rice. Sci Rep **7:** 40641
849 **Singh A, Mittal D, Lavania D, Agarwal M, Mishra RC, Grover A** (2012) OsHsfA2c and OsHsfB4b
850 are involved in the transcriptional regulation of cytoplasmic OsClpB (Hsp100) gene in rice
851 (Oryza sativa L.). Cell Stress Chaperones **17:** 243-254
852 **Sosso D, Luo D, Li QB, Sasse J, Yang J, Gendrot G, Suzuki M, Koch KE, McCarty DR, Chourey**
853 **PS, Rogowsky PM, Ross-Ibarra J, Yang B, Frommer WB** (2015) Seed filling in
854 domesticated maize and rice depends on SWEET-mediated hexose transport. Nat Genet
855 **47:** 1489-1493
856 **Trapnell C, Williams BA, Pertea G, Mortazavi A, Kwan G, van Baren MJ, Salzberg SL, Wold BJ,**
857 **Pachter L** (2010) Transcript assembly and quantification by RNA-Seq reveals unannotated
858 transcripts and isoform switching during cell differentiation. Nat Biotechnol **28:** 511-515
859 **Waadt R, Schmidt LK, Lohse M, Hashimoto K, Bock R, Kudla J** (2008) Multicolor bimolecular
860 fluorescence complementation reveals simultaneous formation of alternative CBL/CIPK
861 complexes in planta. Plant J **56:** 505-516
862 **Walter M, Chaban C, Schutze K, Batistic O, Weckermann K, Nake C, Blazevic D, Grefen C,**
863 **Schumacher K, Oecking C, Harter K, Kudla J** (2004) Visualization of protein interactions
864 in living plant cells using bimolecular fluorescence complementation. Plant J **40:** 428-438
865 **Wang L, Xie W, Chen Y, Tang W, Yang J, Ye R, Liu L, Lin Y, Xu C, Xiao J, Zhang Q** (2010) A
866 dynamic gene expression atlas covering the entire life cycle of rice. Plant J **61:** 752-766
867 **Wang L, Zhou Z, Song X, Li J, Deng X, Mei F** (2008) Evidence of ceased programmed cell death
868 in metaphloem sieve elements in the developing caryopsis of Triticum aestivum L.
869 Protoplasma **234:** 87-96
870 **Wang Y, Xiao Y, Zhang Y, Chai C, Wei G, Wei X, Xu H, Wang M, Ouwerkerk PB, Zhu Z** (2008)
871 Molecular cloning, functional characterization and expression analysis of a novel
872 monosaccharide transporter gene OsMST6 from rice (Oryza sativa L.). Planta **228:** 525-
873 535
874 **Wu X, Liu J, Li D, Liu CM** (2016) Rice caryopsis development II: Dynamic changes in the
875 endosperm. J Integr Plant Biol **58:** 786-798
876 **Xiong Y, Ren Y, Li W, Wu F, Yang W, Huang X, Yao J** (2019) NF-YC12 is a key multi-functional

877 regulator of accumulation of seed storage substances in rice. J Exp Bot **70:** 3765-3780
878 **Xu GY, Rocha PS, Wang ML, Xu ML, Cui YC, Li LY, Zhu YX, Xia X** (2011) A novel rice calmodulin-
879 like gene, OsMSR2, enhances drought and salt tolerance and increases ABA sensitivity in
880 Arabidopsis. Planta **234:** 47-59
881 **Xue W, Xing Y, Weng X, Zhao Y, Tang W, Wang L, Zhou H, Yu S, Xu C, Li X, Zhang Q** (2008)
882 Natural variation in Ghd7 is an important regulator of heading date and yield potential in
883 rice. Nat Genet **40:** 761-767
884 **Yamaguchi M, Ohtani M, Mitsuda N, Kubo M, Ohme-Takagi M, Fukuda H, Demura T** (2010)
885 VND-INTERACTING2, a NAC domain transcription factor, negatively regulates xylem
886 vessel formation in Arabidopsis. Plant Cell **22:** 1249-1263
887 **Yang J, Luo D, Yang B, Frommer WB, Eom JS** (2018) SWEET11 and 15 as key players in seed
888 filling in rice. New Phytol
889 **Yang SD, Seo PJ, Yoon HK, Park CM** (2011) The Arabidopsis NAC transcription factor VNI2
890 integrates abscisic acid signals into leaf senescence via the COR/RD genes. Plant Cell **23:**
891 2155-2168
892 **Young MD, Wakefield MJ, Smyth GK, Oshlack A** (2010) Gene ontology analysis for RNA-seq:
893 accounting for selection bias. Genome Biol **11:** R14
894 **Zhang WH, Zhou YC, Dibley KE, Tyerman SD, Furbank RT, Patrick JW** (2007) Nutrient loading
895 of developing seeds. Functional Plant Biology **34:** 314-331
896 **Zhang Y, Liu T, Meyer CA, Eeckhoute J, Johnson DS, Bernstein BE, Nusbaum C, Myers RM,**
897 **Brown M, Li W, Liu XS** (2008) Model-based analysis of ChIP-Seq (MACS). Genome Biol
898 **9:** R137
899 **Zhang Z, Dong J, Ji C, Wu Y, Messing J** (2019) NAC-type transcription factors regulate
900 accumulation of starch and protein in maize seeds. Proc Natl Acad Sci U S A **116:** 11223-
901 11228